JURASSIC COOLING AGES IN PALEOZOIC TO EARLY MESOZOIC GRANITOIDS OF NORTHEASTERN PATAGONIA: $^{40}AR/^{39}AR$, ^{40}K-^{40}AR MICA AND U-PB ZIRCON EVIDENCE

Carmen I. MARTÍNEZ DOPICO[1,2*], Eric TOHVER[3], Mónica G. LÓPEZ DE LUCHI[1,2], Klaus WEMMER[4], Augusto E. RAPALINI[2,5], Peter A. CAWOOD[6, 7]

[1] *Instituto de Geocronología y Geología Isotópica (INGEIS), Buenos Aires, Argentina. Email:* Carmen.martinez.dopico@gmail.com, deluchi@ingeis.uba.ar

[2] *Consejo Nacional de Investigaciones Científicas y Técnicas (CONICET), Buenos Aires, Argentina.*

[3] *University of Western Australia, School of Earth and Geographical Sciences, Perth, Australia. Email:* eric.tohver@uwa.edu.au

[4] *Geoscience Centre of the University of Göttingen (GZG), Göttingen, Germany. Email:* kwemmer@gwdg.de

[5] *Instituto de Geociencias Básicas, Aplicadas y Ambientales de Buenos Aires (IGEBA), Buenos Aires, Argentina. Email:* rapalini@gl.fcen.uba.ar

[6] *Department of Earth Sciences, University of St. Andrews, North Street, St Andrews, KY16 9AL, United Kingdom. Email:* pac20@st-andrews.ac.uk

[7] *School of Earth, Atmosphere & Environment, Monash University, Melbourne, VIC 3800, Australia*

[*]Corresponding author: *Email:* Carmen.martinez.dopico@gmail.com. Postal address: Intendente Güiraldes 2160, C1428EGA, Ciudad de Buenos Aires, Argentina

ABSTRACT

U-Pb SHRIMP zircon crystallization ages and Ar-Ar and K-Ar mica cooling ages for basement rocks of the Yaminué and Nahuel Niyeu areas in northeastern Patagonia are presented. Granitoids that cover the time span from Ordovician to Early Triassic constitute the main outcrops of the western sector of the Yaminué block. The southern Yaminué Metaigneous Complex comprises highly deformed Ordovician and Permian granitoids cross-cut by undeformed leucogranite dikes (U-Pb SHRIMP zircon age of 254 ± 2 Ma). Mica separates from highly deformed granitoids from the southern sector yielded an Ar-Ar muscovite age of 182 ± 3 Ma and a K-Ar biotite age of 186 ± 2 Ma. Moderately to highly deformed Permian to early Triassic granitoids made up the northern Yaminué Complex. The late Permian to early Triassic (U-Pb SHRIMP zircon age of 252 ± 6 Ma) Cabeza de Vaca Granite of the Yaminué block yielded Jurassic mica K-Ar cooling ages (198 ± 2 Ma, 191 ± 1 Ma, and 190 ± 2 Ma). At the boundary between the Yaminué and Nahuel Niyeu blocks, K-Ar muscovite ages of 188 ± 3 and 193 ± 5 Ma were calculated for the Flores Granite whereas the early Permian Navarrete granodiorite, located in the Nahuel Niyeu block, yielded a K-Ar biotite age of 274 ± 4 Ma. The Jurassic thermal history is not regionally uniform. In the supracrustal exposures of the Nahuel Niyeu block, the Early Permian granitoids of its western sector as well as other Permian plutons and Ordovician leucogranites located further east show no evidence of cooling age reset since mica ages suggest cooling in the wake of crystallization of these intrusive rocks. In contrast, deeper crustal levels are inferred for Permian-Early Triassic granitoids in the Yaminué block since cooling ages for these rocks are of Jurassic age (198-182 Ma). Jurassic resetting is contemporaneous with the massive Lower Jurassic Flores Granite, and the Marifil and Chon Aike volcanic provinces. This intraplate deformational pulse that affected northeastern Patagonia during the Early Jurassic (Sinemurian- Pliensbachian) was responsible for the partial (re)exhumation of the mid-crustal Paleozoic basement along reactivated discrete NE-SW to ENE-WSW lineaments and the resetting of isotopic systems. This new thermochronological data indicates that Early Permian magmatic rocks of the Nahuel Niyeu block were below 300°C for ca. 20 Ma prior to the onset of the main magmatic episode of the Late Permian to Triassic igneous and metaigneous rocks of the Yaminué block.

Keywords: *Patagonia; magmatism; Paleozoic basement; reset crystallization ages; cooling ages*

1. INTRODUCTION

The thermal history of magmatic rocks can provide important insights into the tectonic processes that lead to the exhumation of plutonic rocks. In the present paper we explore part of the cooling history of granitoids of the northeastern corner of the North Patagonian Massif. The late Paleozoic to early Mesozoic tectonic evolution of Patagonia and its relation with the continental blocks located to the north of the Río Colorado is not well established (figure 1a). Despite much progress in the last decade concerning the geological evolution of northern Patagonia, there are still open questions due to a paucity of well dated rocks in the region. Recent studies provide evidence that the northeastern sector of the North Patagonian Massif is either an allochthonous block that collided with Gondwana in the late Paleozoic (Ramos, 1984; Chernicoff et al., 2013) or was already part of Gondwana (Pankhurst et al., 2006; Gregori et al., 2008, 2013) but was remobilized following rifting during early Paleozoic times (López de Luchi et al., 2010; Rapalini et al., 2010, 2013). The collisional hypothesis is not fully supported by existing evidence, and many questions remain regarding geochemical signature and tectonic significance of the late Paleozoic to Triassic magmatism, the timing of the collision, and the metamorphic overprint in terms of evolving P-T conditions preserved in the affected rocks. The best record of the late Paleozoic-Early Triassic tectonic evolution of the North Patagonian Massif is found in rocks outcropping along state road 23 and further south between the towns of Yaminué and Valcheta (figure 1b) (Pankhurst et al., 2014). Widespread Permian to middle Triassic magmatic rocks dominate this region, with magmatism separated into two main groups of granitoids: the older episode dated at ca. 280 Ma, the Early Permian granitoids (Navarrete Plutonic Complex, Pankhurst et al., 2006, 2014; López de Luchi et al., 2010) and the younger event (<260 to 245 Ma) that is made up of several igneous complexes: the intensely deformed Yaminué Metaigneous Complex (López de Luchi et al., 2010; Chernicoff et al., 2013; Pankhurst et al., 2014), the Cabeza de Vaca Granite (López de Luchi et al., 2010), the Ramos Mexia Igneous Complex and the Madsen Tonalite (López de Luchi et al., 2015) (figure 1b). The late Permian-Middle Triassic rocks of the Yaminué Metaigneous Complex (Chenicoff et al., 2013; Pankhurst et al., 2014; López de Luchi et al., 2015) are inferred to represent the implied syncollisional and postcollisional stages of the cycle. On the other hand, Ordovician ages (~460 Ma) have been determined for metaigneous rocks located at the southern area of the Yaminué Metaigneous Complex (Rapalini et al., 2013).

The youngest geological unit in the region is the Triassic to Jurassic (?) Treneta Volcano- Plutonic Complex (Caminos et al., 2001). This complex has been interpreted as the result of orogenic collapse that triggered the opening of the Neuquén basin in northwestern Patagonia (Franzese and Spalletti, 2001). These events are

correlated with extensional episodes associated with massive silicic magmatism along Patagonia and the Antarctic Peninsula (Pankhurst et al., 2000).

The aims of this contribution are a) to provide new U-Pb crystallization zircon ages and Ar/Ar and K-Ar mica cooling ages for the Yaminué Metaigneous Complex, Cabeza de Vaca Granite, Navarrete Plutonic Complex and Flores Granite of the Treneta Volcano-Plutonic Complex, b) to integrate the new data with all published geochronological and geological data, and c) to present a geodynamic model for the late Paleozoic to Jurassic deformational and magmatic events of that occurred in the northeast of the North Patagonian Massif.

2. GEOLOGICAL SETTING

The northeastern sector of the North Patagonian Massif consists of northeast-southwest trending stacked blocks of basement that represent different segments of Paleozoic crust (figure 1) (López de Luchi et al., 2010; Chernicoff et al., 2013; Gregori et al., 2013). At least two peaks of metamorphic activity (Middle Ordovician and Permian) have been ascribed to this region, including regional deformation as well as multiple episodes of calc-alkaline magmatism during Ordovician, Permian, Triassic and Jurassic times (Caminos, 2001; Rapalini et al., 2013; Chernicoff et al., 2013; Pankhurst et al., 2014 among others). Field evidence indicates that in every case the magmatism postdates the peak metamorphic conditions (Gozálvez, 2009a; López de Luchi et al., 2010; Greco et al., 2015). From west to east these blocks are known as the Yaminué, Nahuel Niyeu (figure 1b) and Gonzalito/Tembrao blocks. The blocks themselves are separated by steep NE-SW and NW-SE shear zones and/ or faults (Von Gosen, 2003) or lineaments that bound gravimetric and aeromagnetic anomalies (Croce et al., 2009; Lince Klinger et al., 2010, 2014; Chernicoff et al., 2013; figure 1b). These anomalies coincide with the exposures of the Triassic to Jurassic (?) Treneta Volcanic- Plutonic Complex. This contribution will focus on the Yaminué and Nahuel Niyeu blocks; the Gonzalito block (Giacosa, 1997; González et al., 2014; Gregori et al., 2008, 2013) to the east will not be discussed.

The oldest geological unit of the area, the early Cambrian Tardugno Granodiorite (U-Pb SHRIMP ages on igneous zircons between 522 ± 3 and 529 ± 4 Ma; Rapalini et al., 2013; Pankhurst et al., 2014) is sandwiched between the Yaminué and the Nahuel Niyeu blocks. The body displays a porphyritic, coarse-grained, biotite-bearing gneissic fabric with a granodioritic- monzogranitic chemistry. The boundaries of the Tardugno Granodiorite are strongly sheared, and the body is locally intruded by the 252 ± 3 Ma Madsen Tonalite

(Pankhurst et al., 2014; López de Luchi et al., 2015) and covered by the early Mesozoic Treneta volcanic rocks and fine grained leucogranites (figure 1b).

2.1 Yaminué Block

The Yaminué block lies in the western portion of the study area (figure 1b). This block exposes the deepest section of early Paleozoic crust in the region. The main units correspond to (a) the intensively deformed Yaminué Metaigneous Complex, (b) the Cabeza de Vaca Granite and (c) the Ramos Mexia Igneous Complex (López de Luchi et al., 2010, 2015; Rapalini et al., 2013; Pankhurst et al., 2014). The latter is locally covered by ignimbrites of the Treneta Volcanic-Plutonic Complex and intruded by epizonal Jurassic leucogranites that could belong to the Flores Granite (Caminos, 2001; Pankhurst et al., 1993).

(a) *The Yaminué Metaigneous Complex*: The term "Yaminué Complex" was originally employed by Chernicoff and Caminos (1996) to include all the deformed intrusive and metamorphic units of the area. The complex is made of sheet-like bodies of a coarse to medium grained porphyritic granodiorite-monzogranite, and less common tonalite (López de Luchi et al., 2010). These units are separated by sub-concordant sheets of tonalitic biotite-orthogneiss, and pegmatoid to porphyritic leucogranite. Locally undeformed biotite leucogranite cuts across the penetrative fabric. The complex was originally considered to be Precambrian in age, on the basis of poor-quality radiometric dating (Caminos et al., 1994). This view began to change with the reports by Basei et al. (2002) and, after, by Pankhurst et al. (2014), who re-examined localities and presented late Permian to early Triassic SHRIMP U-Pb zircon igneous ages (*ca.* 250 Ma, see figure 1b). These results complemented the findings of Chernicoff et al. (2013), who reported a U-Pb SHRIMP zircon age for a tonalite orthogneiss of 261.3 ± 2.7 Ma. On the other hand, U-Pb SHRIMP ages of a strongly foliated tonalite/granodiorite orthogneiss of the classical locality of the Yaminué Complex at Puesto Peynecura (southern sector) (figure 1b) yielded a crystallization age of 466.6 ± 6.7 Ma (Rapalini et al., 2013). These data suggest that the "Yaminué Complex" includes at least two pulses of magmatic activity: Ordovician (ca 470 Ma) and Permian (260-250 Ma). The southern Yaminué Metaigneous Complex (López de Luchi et al., 2015). comprises N-S striking sheets of orthogneisses that consist of coarse to medium-grained porphyritic biotite-granodiorite-tonalite (López de Luchi et al., 2010) that occur in shallowly east or west dipping sheets. The fabric of the orthogneiss sheets are sub-concordant with medium-grained, leucogranites, which cross-cuts the gneissic foliation in some outcrops. Further south of the main outcrops, near Puesto Peynecura (figure 1 b), small blocks of white and black marbles as well as rare amphibolite bodies are in fault contact with the orthogneisses. Although these metamorphic

lithologies are scarce in Valcheta- Yaminué area, their abundance is greater in the east, in the Mina Gonzalito Block, where the main metamorphic peak has been constrained to *ca*. 472 Ma (U-Pb SHRIMP zircon, Pankhurst et al., 2006). At Puesto Peynecura, Chernicoff et al. (2013) described a metaclastic biotite-plagioclase-muscovite gneiss that exhibits a strong inheritance of Ordovician magmatic zircons (maximum probability peak at 475 Ma) with overprinting metamorphic rims of Ordovician and Devonian age (main maximum probability peaks at 450 Ma and 380 Ma). The youngest single zircon from this rock was dated as 318 ± 5 Ma (U-Pb SHRIMP dating, Chernicoff et al., 2013).

The northern sector of the Yaminué Metaigneous Complex has been dated as late Permian to Middle Triassic (260-245 Ma) (Tohver et al., 2008; Chernicoff et al., 2013; Pankhurst et al., 2014). These rocks encompass shallowly NE-dipping sheet-like bodies of variably foliated biotite-bearing porphyritic granodiorite, tonalite, biotite ± amphibole granodiorites, and biotite monzogranites layers (López de Luchi et al., 2010). The sheet-like bodies are separated by sub-concordant sheets of light pink fine-grained biotite bearing leucogranites and some pegmatite dikes.

(b) *Cabeza de Vaca Leucogranite:* It is composed of non-foliated plutons as well as foliated leucogranitic sheets and dikes that occur as either isolated or concordantly intruding the granodiorite-monzogranite rocks of the Yaminué Metaigneous Complex (López de Luchi et al., 2010). These sheets were deformed into tight folds with northwest to north trending axes (Chernicoff and Caminos, 1996) and later affected by open folds with NE trending axes.

(c) *Ramos Mexia Igneous Complex:* The complex is made up by the Robaina Granite and the Guanacos Granite, which are variably foliated biotite monzogranites and biotite amphibole granodiorites (López de Luchi et al., 2010). Rock fabrics that developed under ductile conditions were identified in the Robaina Granite towards the western border close to the western outcrops of the Yaminué Metaigneous Complex.

2.2 Nahuel Niyeu Block

Exposures of this block extend from the lower reaches of Treneta Creek to the east and southeast to the town of Valcheta. The most conspicuous unit in this area is the low to medium grade metavolcanic and metaclastic rocks of the Nahuel Niyeu Formation (Cagnoni et al., 1993; Caminos, 2001; Martínez Dopico et al., 2014; Greco et al., 2015). Provenance studies are consistent with a Neoproterozoic to Early Paleozoic tectonic setting associated with subduction in a continental margin or island arc (Cagnoni et al., 1993; Pankhurst et al., 2006). Maximum

depositional ages of the unit at Puesto Navarrete and Puesto Aranda are ca. 515 Ma (very low grade metamorphic metaclastic rocks) based on U-Pb SHRIMP detrital zircon dating (Pankhurst et al., 2006; Rapalini et al., 2013). Towards the east, the metamorphic grade increases and the metaclastic and metavolcanic rocks are intruded by several Late Cambrian (?) to Ordovician leucogranites (Gozálvez, 2009a; Martínez Dopico et al., 2010a) and covered by Silurian-Devonian iron-bearing sedimentary rocks of Sierra Grande Formation (Caminos 1981; Zanettini 1981; Uriz et al., 2011). The Early Permian Navarrete Plutonic Complex (281 ± 3 Ma; Pankhurst et al., 2006) intrudes the supracrustal sequence of the Nahuel Niyeu Block (Caminos, 1983; López de Luchi et al., 2010; Pankhurst et al., 2014) at its type locality near Puesto Navarrete. Since the Navarrete Complex *sensu lato* encompasses large geochemical variations and styles of emplacement (López de Luchi et al., 2010), we have preferred to restrict this complex to its type area. An erosional unconformity (Caminos, 2001) separates these rocks from the Treneta Volcanic-Plutonic Complex that is made up by the Triassic to Jurassic (?) andesites, rhyolitic and dacitic ignimbrites of the Treneta Formation and the early Jurassic undeformed biotite-bearing Flores Granite, which represents the late stage of the epizonal plutonic activity in the region. No age has been obtained for the Treneta volcanic rocks. However, an andesitic dike swarm in the Mina Gonzalito area (figure 1a) yielded a Middle Triassic age (243.6 ± 1.7 Ma, González et al., 2014). Pankhurst et al. (1993) calculated a whole rock Rb-Sr isochron age of 188 ± 3 Ma for the Flores Granite based on samples from the coarse and fine grained facies of the body. Therefore, this intrusive event is coeval with the rhyolitic flows of the Marifil Volcanic Complex (Pankhurst and Rapela, 1995; Féraud et al., 1999; Márquez et al., 2010).

3. SAMPLING STRATEGY AND GEOCHRONOLOGICAL METHODS

Five to ten kilograms samples were collected at nine localities (two U-Pb zircon and nine K-Ar or Ar/Ar mica dating) of the main Paleozoic to early Mesozoic plutonic units including the southern and northern Yaminué Metaigneous Complex, the Cabeza de Vaca Granite, the Navarrete Plutonic Complex (figure 1b), and the fine grained facies of the Flores Granite.

3.1. K-Ar and Ar-Ar Dating

Selected samples for K-Ar and Ar-Ar dating were crushed in a steel jaw crusher and sieved to isolate the 300–400 μm size fraction. These fractions were carefully processed by magnetic separation. Mica grains from each sample were handpicked under a binocular microscope. The purity of the mineral separates is > 99%. Biotite and

muscovite were purified and ground in pure alcohol using arough surface porcelain mortar and pestle to remove potential altered rims that might have suffered a loss of Ar or K.

K-Ar mica dating was performed in the Geowissenschaftliches Zentrum of the University of Göttingen (Germany). Details of the K-Ar analyses of the laboratory are given in Wemmer (1991). For all samples, atmospheric ^{40}Ar was below 5%, the isotopic composition of Ar was measured with a Thermo-Scientific ARGUS VI ™ multi-collector noble gas mass spectrometer. K_2O values were determined in duplicate using a BWB-XP ™ flame photometer. $^{40}Ar/^{39}Ar$ analyses were carried out in at the Western Australian Argon Isotope Facility at Curtin University. Procedures and applied corrections for the Ar-dating are those described in Tohver et al. (2012). Detailed data are available in Appendix A.

3.2 U-Pb zircon SHRIMP dating

Zircon were extracted by crushing and sieving of samples, followed by Wilfley table and heavy liquid separation. Separated grains were handpicked using a binocular microscope, and mounted in epoxy resin for polishing prior to scanning electron microscope and cathodoluminescence imaging. The epoxy mounts were gold-coated to have a uniform electrical conductivity for SHRIMP analysis. The zircon standard used was BR266 (Stern, 2001). The isotopic composition of the minerals was determined using the SHRIMP II housed at Curtin University. The common Pb correction was carried out using the measured amount of ^{204}Pb. Isotope data was reduced using the SQUID2 software (Ludwig, 2009). Between 10 and 11 zircon grains were dated for each sample, discordant and inherited zircon data was discarded. Data was plotted on concordia diagrams using the Concordia Age tool of Isoplot 4.16 software (Ludwig, 2012), with 2-sigma error ellipses on the concordia plots and all the ages reported at the 2-sigma confidence level in the text. The parameters of the sessions were presented in Rapalini et al. (2013). The data are available in Appendix B.

4. RESULTS AND INTERPRETATION OF THE COOLING AGES

The K-Ar and Ar-Ar mica as well as the U-Pb SHRIMP zircon ages are presented in Table 1. Three new K-Ar cooling ages on muscovite for the Yaminué Block yielded Early Jurassic ages. The first sample was coarse grained foliated garnet-muscovite bearing leucogranite from the southern sector in the area of Puesto Peynecura (sample V79-1 - Yaminué Metaigneous Complex). An U-Pb SHRIMP zircon age identified the crystallization age for these rocks as 466.6 ± 6.7 Ma (Rapalini et al., 2013) (figure 2a, b). Muscovite grains define the shallow

ESE dipping foliation, which is concordant with the fabric of the granodiorites and tonalites. Muescovite separated from this sample yielded a K-Ar age of 182.4 ± 2.9 Ma. Sample V69, a separate of muscovite booklets of pegmatitic miaroles in a foliated NE trending leucogranite dike that intrudes the Robaina Granite of the Ramos Mexia Plutonic Complex, gave an age of 190.1 ± 2.0 Ma. Muscovite concentrates of sample Val55, yielded a K-Ar age of 198.2 ± 2.2 Ma. This sample corresponds to a medium to coarse grained sheeted-like leucogranite in which muscovite defines the NW-SE foliation, which is slightly discordant respect to the main WNW-ESE trending fabric of the host granodiorite, both locally folded around an ENE trending axis. Leucogranites interlayered with granodiorites and tonalites of the northern Yaminué Metaigneous Complex are interpreted as belonging to the Cabeza de Vaca granites by López de Luchi et al. (2010). Muscovite grains from an undeformed monzogranite of the Navarrete Plutonic Complex (V75) sampled nearby Puesto Aranda (30 km south of Puesto Navarrete) gave a K-Ar age of 274.3 ± 4.1 Ma. Muscovite from two pegmatitic miaroles (V27b and V8E) were obtained of the Flores Granite, and yielded ages of 188.2 ± 2.9 Ma and 193.3 ± 4.5 Ma, respectively. These muscovite booklets up to 3-4 cm long together with K-feldspar and minor plagioclase made up the miaroles in the fine grained leucogranite facies of this pluton.

Muscovite and biotite grains selected for $^{40}Ar/^{39}Ar$ dating correspond to the Nahuel Niyeu Formation and the Southern Yaminué Complex and Cabeza de Vaca Granite (Table 1, figure 2b, d, f). V79 is a strongly foliated granodiorite at Puesto Peynecura, with a SHRIMP U-Pb zircon age of 466.6 ± 6.7 Ma reported by Rapalini et al. (2013) (figure 2a). The biotite plateau indicates an age of 185.8 ± 1.5 Ma (figure 2b). It is important to highlight that this sample is interlayered with the leucogranite sampled for K-Ar (V79-1), with a K-Ar muscovite cooling age of 182.4 ± 2.9 Ma. V58 is a massive biotite bearing granite of the Cabeza de Vaca Granite near Estancia Cabeza de Vaca in the northernmost corner of the block. U-Pb SHRIMP zircon crystallization age of this rock is 252.6 ± 2.8 Ma whereas the $^{40}Ar/^{39}Ar$ biotite plateau age is 191.4 ± 1.4 Ma (figure 2c, d). In Puesto Navarrete, muscovite blasts from the contact aureole in the low grade metasediments of the Nahuel Niyeu Formation with the Navarrete Plutonic Complex gave a $^{39}Ar/^{40}Ar$ plateau age of 264.8 ± 1.9 Ma (figure 2f).

5. DISCUSSION

Available and new U-Pb zircon SHRIMP dating in concert with K-Ar and Ar-Ar thermochronology on muscovite and biotite allow characterising the crystallization and thermal history of the NE sector of the North Patagonian Massif. These new age data provide geo-thermochronological constraints and illustrate the nature of

orogenic processes (e.g., Kirscher et al., 2003; Steenken et al., 2004; Hansma et al., 2015). K-Ar white mica ages document the closure temperature for 'normal' fine to coarse-grained rocks below 350 ± 50 °C (Purdy and Jäger, 1976). More recently, Harrison et al. (2009) conducted diffusion experiments on muscovite and indicated a closure temperature (Tc) of 425 ºC for a 100 µm radius grain cooling at 10 ºC/Ma at 10 kbar (Tc = 405ºC at 5 kbar). The typical closure temperature for biotite in the K-Ar isotopic system is lower, around 300 °C. The dependence of the closure temperature on the grain-size of the mica (McDougall and Harrison, 1999) must be considered for muscovite-booklets of pegmatitic grain-size because as the effective diffusion lengths of Ar loss are high, effective closure temperatures are significantly above the 'commonly accepted' values (Büttner et al., 2005). This effect might be enhanced by the absence of pervasive deformation of the pegmatite and the lack of recrystallization of the booklets. This would be the case for the data obtained for the non-deformed mica of the miaroles of the Flores Granite. Therefore, we interpret these ages as a primary cooling for the Flores Granite. In contrast, white mica and biotite ages obtained from several sectors of the highly deformed rocks of the Yaminué Complex and dikes intruding Ramos Mexía Complex more likely represent a resetting related to a deformational rather than a protracted cooling as suggested when Lower Jurassic Ar-Ar mica dating is compared to the Permian to Early Triassic U-Pb zircon crystallization ages obtained herein and by Pankhurst et al. (2006, 2014) and Rapalini et al. (2013) among others (figure 1 b). Since the main deformational event that controlled pervasive ductile high temperature deformation of part of these rocks is, in most cases, synkinematic, it does not seem to be Jurassic in age. Therefore our new set of ages provides evidence of different deformational and magmatic events that affected from a local to a regional scale the late Paleozoic to Triassic units of the North Patagonian Massif. All the geochronological information published for the study area is displayed in figure 3.

5.1 Cooling and deformation in the Yaminué block

Our new zircon ages, together with recently published data from the southern Yaminué Metaigneous Complex indicate three periods of significant geological activity. Regional basement comprises Ordovician igneous rocks to biotite-bearing paragneisses with inherited detritus from Devonian to Carboniferous sources. Finally, late Permian to Middle Triassic igneous intrusions are regionally widespread (figure 3). The Ordovician magmatic episode has been dated by Rapalini et al. (2013) at Puesto Peynecura as 466.6 ± 6.7 Ma. The precise age of crystallization is clouded by some dispersion of ages from individual zircon grains, perhaps reflecting differential Pb loss during later magmatic/metamorphic episodes. The presence of inherited Ordovician-aged zircon in < 318 Ma biotite paragneiss (Chernicoff et al., 2013) from Puesto Peynecura might reflect the short

293 detrital transport distances from a proximal Ordovician magmatic source (figure 4). This Ordovician
294 crystallization age cluster is coincident with the age of the metamorphic episode dated in the Gonzalito
295 Metamorphic Complex and the hybrid magmatism of the Punta Sierra Plutonic Complex (Gonzalito Block,
296 Pankhurst et al., 2006) as well as with the leucogranite and granites of the Valcheta Pluton (Nahuel Niyeu Block;
297 Gozálvez, 2009a; Martínez Dopico et al., 2010b). The < 318 Ma age of the biotite paragneiss (Chernicoff et al.,
298 2013) shows a Devonian to Carboniferous magmatic or metamorphic detrital supply which could be coming
299 from sources present in the western Patagonian region (Pankhurst et al., 2006). The 318 Ma age is interpreted as
300 the maximum depositional age for the rock, which constraints the metamorphic and deformational event as
301 younger than 318 Ma and synchronous with the intrusion of the northern Yaminué Complex that is considered to
302 be syn-kinematic. U-Pb zircon age dating for Yaminué Granites is broadly bracketed between late middle
303 Permian and Middle Triassic (Figure 1b; Chernicoff et al., 2013; Tohver et al., 2008), but most of the
304 crystallization ages are ca 250 Ma (this paper, Pankhurst et al., 2014; figure 4).
305 Thermobarometric constraints on the emplacement of a 251 ± 2 Ma foliated granodiorite of the northern
306 Yaminué Complex (Pankhurst et al., 2014) suggest *ca* 5-6 Kbar (Rapalini et al., 2010). On the other hand, the
307 245.2 ± 1.5 Ma Robaina facies of the Ramos Mexia Complex in the northeastern part of the block is emplaced in
308 the Cambrian metasedimentary rocks of the Nahuel Niyeu Formation and develops a contact aureole with
309 andalusite blasts (ca 2 Kbar). Both units exhibit ~188 Ma Early Jurassic mica cooling ages (figure 4), which
310 suggests that these two complexes were exhumed at this time.
311
312 **5.2 Cooling and Deformation in the Nahuel Niyeu Block**
313 Mica cooling ages provided by K-Ar and $^{40}Ar/^{39}Ar$ indicate that these units were at the ca. 350º C isotherm in the
314 middle Permian. The new muscovite cooling age herein provided for a sample of the Navarrete Plutonic
315 Complex north of Puesto Aranda is 274.3 ± 4.1 Ma. At the type locality of this unit, a SHRIMP age on zircon of
316 283 ± 2 Ma for an undeformed granodiorite intruding very low grade phyllites (mottled schists) of the Nahuel
317 Niyeu Formation was calculated by Pankhurst et al. *(*2006). Muscovite grains from these schists yielded
318 $^{40}Ar/^{39}Ar$ age of 264.8 ± 1.9 Ma, confirming thermal overprint associated with Early Permian magmatism
319 represented by the Navarrete Plutonic Complex as proposed by Pankhurst et al. (2006). If so, regional cooling of
320 the Navarrete Plutonic Complex to ~300ºC would have taken place over ca. 20 Ma. Zr thermometry of the
321 Navarrete Plutonic Complex indicates temperatures around 780-800ºC (Rapalini et al., 2010) which implies a
322 cooling rate of ca. 30 ºC/Ma for the period 283-265 Ma. Because the contact metamorphic assemblages in the

Nahuel Niyeu Formation include andalusite, now present as sericite pseudomorphs, the Navarette Plutonic Complex is considered to have intruded at shallow depths. Thus, the late Paleozoic history of magmatism for the Nahuel Niyeu block is one of shallow intrusions ending at ca. 260 Ma. Subsequent reactivation in the Jurassic resulted in the deposition of Marifil Formation that discordantly overlies the Nahuel Niyeu Formation. The crystallization age range obtained for all the late Permian to Triassic units in the Yaminué Block do not overlap the time span (283-260 Ma) proposed for the Navarrete Plutonic Complex (Pankhurst et al., 2006, and this paper), San Martín Pluton (figure 1, Gozálvez, 2009b), or for the Pailemán Plutonic Complex (located further east of the studied area; Giacosa, 1999; Grecco and Gregori, 2011).

5.3 Regional framework for the Lower Jurassic deformational event

Thermo-mechanical overprinting of the Yaminué block is recorded by Lower Jurassic cooling ages in mica. The K-Ar ages of 182.4 ± 2.9 Ma from deformed muscovite is similar to the Ar-Ar 185.6 ± 1.5 Ma biotite cooling age of the foliated granodiorite (Table 1). Since cooling ages are Lower Jurassic (*ca.* 188 Ma) at different localities of the Yaminué Metaigneous Complex and Cabeza de Vaca Granite, the simplest hypothesis is that cooling was protracted and very slow or, alternatively, that this crustal segment might have experienced a Jurassic uplift and at least partial exhumation as indicated by the outcrops of the Robaina facies that are partially covered by the Treneta Volcanic-Plutonic Complex. Given the difference in closure temperature for the dated minerals (≈ 280°C for biotite, 300-350º C, Harrison et al., 1985; Dahl, 1996; 425°C for muscovite, Harrison et al., 2009), the concordance of Ar-Ar and K-Ar ages indicates relatively fast cooling of mylonitized gneisses and granodiorites, as well as the less deformed granites. In this context, it is suggested that fast cooling after a period of quiescence could have been triggered by deformation with partial removal of the foot wall rocks (Yaminué Metaigneous Complex), promoting fast ascent of isotherms to upper crustal levels and the resetting of the isotopic system of the micas.

The next recorded magmatic event is the emplacement of the undeformed epizonal Flores Granite, located in the boundary between the Yaminué and Nahuel Niyeu blocks. The ca. 190 Ma Flores Granite (Rb-Sr WR isochron) would be coeval with the silica rich Marifil Complex, according to Jurassic ages presented here and those previously provided by Pankhurst et al. (1993). The Lower Jurassic ages for muscovite booklets of the Flores Granite support the WR Rb-Sr isochrons because their closure temperature would be around 500ºC. All these data are minimum ages of intrusion, which are expected to be close to the crystallization age for shallow intrusions into cool upper crust. Our field observations in areas close to the samples that were dated indicate that

fine grained pink-biotite leucogranites intrude coarse grained facies assigned to the same unit but from which precise ages are lacking. This fact fosters an older age for the coarse grained facies, in agreement with other similar leucogranite units in the North Patagonian Massif as the Calvo Granite (250 Ma, Pankhurst et al., 2006) or even, Cabeza de Vaca Granite of the Yaminué Block (López de Luchi et al., 2010).

5.4 Regional Synthesis

A late Ordovician or early Silurian episode of exhumation occurred across the study region since magmatic Ordovician zircons are the main detrital contribution not only in the Sierra Grande Formation (Uriz et al., 2011), which overlies the Nahuel Niyeu Formation, but also in the Yaminué block in the medium grade metaclastic rocks that host the Yaminué Metaigneous Complex (Rapalini et al., 2013) (figure 3). After this episode each block shows an independent evolution. Granitoids of the Navarrete Plutonic Complex in the Nahuel Niyeu block were at ca. 280-300 ºC in the middle Permian whereas the granitoids of the Yaminué block (re)attained this temperature in the Jurassic. The cooling was faster in the Nahuel Niyeu block and the 274-260 Ma cooling ages would correspond to the beginning of a magmatic gap in high levels of the crust that would extend up to the early Jurassic.

The Yaminué block records the track of Devonian and Carboniferous sedimentation (374 to 395 Ma, Tohver et al., 2008; Chernicoff et al., 2013, respectively) and/or later metamorphism at 320 Ma (Chernicoff et al., 2013) as shown by the detrital zircons of biotite paragneisses that host the Yaminué granites. The comparison of the probability density plots (figure 4) indicates the inheritance is unequivocally Ordovician (main probability density peaks at ca. 460 Ma, and minor at ca. 380 Ma and 530 Ma). A possible igneous source for the 380-395 Ma detrital contribution could be tracked to the westernmost part of the North Patagonian Massif (San Martín de los Andes Tonalite) or granites near Gastre (Pankhurst et al., 2006; figure 1a). As Chernicoff et al. (2013) indicated, although there is no magmatic record ca. 320 Ma in the northeastern sector of the North Patagonian Massif, further southwest, a magmatic calk-alkaline arc in Paso del Sapo, Cordón del Serrucho and part of the Sierra de Mamil Choique, exhibits a clear magmatic record of an age range between 330-280 Ma (Pankhurst et al., 2006).

If metamorphism in the Yaminué block is synchronous with deformation as suggested by the synkinematic emplacement age of northern Yaminué Metaigneous Complex, the event would be bracketed between 252 and 248 Ma. The 10 Ma discrepancy between this cluster and the age of Chernicoff et al. (2013) of 261 ± 3 Ma U-Pb SHRIMP zircon dating from an outcrop apparently less than 5 km away from Pankhurst et al. (2014) U-Pb

SHRIMP dating localities, is still not easy to explain unless the interplay between emplacement and deformation would be more complex. No record of metamorphism of this age range is found in the Nahuel Niyeu Formation (Pankhurst et al., 2006), however, this could be biased by the exposed crustal level.

The ~261 and ~248 Ma episode of widespread synkinematic magmatism of the northern Yaminué Metaigneous Complex is associated with leucogranite intrusions (~252 Ma, Cabeza de Vaca Granites). Evidence for this event is absent from the Nahuel Niyeu supracrustal block but magmatism of this age is found in the Madsen Tonalite, which intrudes the Tardugno granodiorite (Pankhurst et al., 2014). A possible explanation for the lack of late Permian-Triassic magmatism in the Nahuel Niyeu block is provided by the Early Permian cooling age found in the Navarrete Plutonic Complex, which suggest the exposed level of the crust was below 300° C isotherm in the Late Permian. Besides the evidence that Yaminué and Nahuel Niyeu blocks expose different crustal levels, different thermobarometric data for the complexes of the two blocks support this idea. The Navarrete Plutonic Complex yielded 2.1 ± 0.5 kbar (sample V74, Rapalini et al., 2010) and 2.5-3.1 ± 0.5 kbar (Musters Pluton, López de Luchi et al., 2013), whereas 5.1 ± 0.6 kbar were calculated for the interlayered unit of the Ramos Mexía Complex. These differences are consistent with the gravimetric model that suggests around 10 km of uplifting of Yaminué block with respect to the outcrops of the Nahuel Niyeu block (Lince Klinger et al., 2010). In this case, cooling ages from micas would reinforce this difference in crustal levels because only the deeper seated early Permian to early Triassic intrusions of the western block might have recorded the Jurassic resetting.

Circa 80 km to the southeast of Valcheta town, in the Mina Gonzalito block, highly deformed S-type synkinematic magmatism is dated at ~260 Ma in the Tembrao area (^{39}Ar-^{40}Ar ages in Grecco and Gregori, 2011, Tohver et al., 2008). Moreover, hydrothermal fluids have been classically proposed as responsible for age and magnetic resetting during Permian (~260 Ma) and Jurassic times (~190 Ma) in several Ordovician, Permian and Jurassic igneous rocks in the easternmost sector of the North Patagonian Massif, close to Sierra Grande, Mina Gonzalito and Las Grutas areas (Busteros et al., 1998; Aragón et al., 1999; Sato et al., 2004; Varela et al., 2009; Tomezzoli et al., 2013), perhaps associated to the development and/or later extensional reactivation of the El Jagüelito Shear Zone as well as other NW-SE shear zones (Giacosa, 1997; 2001).

6. CONCLUDING REMARKS

The new cooling and crystallization age data presented herein provide clear evidence for the resetting of several Paleozoic to early Mesozoic intrusive units exposed in the northeastern North Patagonian Massif during the

Jurassic (198-182 Ma). This set of ages (~190 Ma) is located in the westernmost part of the area, Yaminué block, where early and late Paleozoic to Early Triassic deeper crustal levels are exposed. In addition, one cooling age of 274 ± 4 Ma confirms an early Permian crystallization age for an undeformed monzogranite in the eastern Nahuel Niyeu block. At present, no evidence for resetting has been found in Nahuel Niyeu block. There, the Jurassic age of the fine grained facies of the undeformed Flores granite has been confirmed and is likely to represent the primary cooling of the pluton. Magmatic ages around ~190 Ma for part of the Flores Granite are consistent with the intraplate Lower Jurassic magmatic event (V1- between 178 and 188 Ma; Marifil Volcanic Event: Pankhurst et al., 2000) related to the westward spreading Karoo thermal anomaly (Jourdan et al., 2005) that affected the North Patagonian and the Deseado massifs. This massive Jurassic magmatic event might have also triggered an intraplate deformational pulse (evidenced by the deformed muscovite grains of the Ordovician rocks of the Yaminué Complex) that could be responsible for the (re)exhumation and deformation of part of the Paleozoic basement of the westernmost Yaminué block through the reactivation of discrete fragile NE-SW to ENE-WSW fault systems and related shear zones as well as the resetting of isotopic systems (190-180 Ma). The Jurassic reactivation of previous late Permian to Triassic NE-SW shear zones related to the amalgamation of the Patagonia blocks, might have led to the current level of crustal exposure. Thus, the timing and duration (between 190 and 180 Ma) of localized intraplate deformation and isotopic reset of low temperature isotopic systems (K-Ar, Ar-Ar and, presumably, Rb-Sr) in the Paleozoic to Triassic basement of the northeastern Patagonia closely overlaps in time with discrete episodes of contraction described in Patagonia. Other evidence of Jurassic intraplate deformation are referred in the wake of uplift of the Huincul High, NW of Patagonia (Naipauer et al., 2012) and the discrete events of tectonic inversion of the West-Gondwana break up related depocenters in the Deseado Massif (Navarrete et al., 2016).

ACKNOWLEDGMENTS

We thank two anonymous reviewers for their detailed comments and W.-C. Dullo for editorial handling. C.M.D. would like to thank F. Jourdan, T. Luppo and F. Narduzzi for discussions on a draft of the paper. University of Buenos Aires (PICTUBACYT X183), CONICET and ANPCYT (PICT20131162) financial support is acknowledged.

443 **REFERENCES LISTED IN THE TEXT**

444 Aragón E, Dalla Salda L, Varela R, Benialgo A. (1999). Jurassic resetted ages of Gonzalito SEDEX deposit,
445 northeastern Patagonia. II South American Symposium on Isotope Geology I: 7-10

446 Basei MAS, Varela R, Sato AM, Siga Jr O, Llambías EJ (2002). Geocronología sobre rocas del Complejo
447 Yaminué, Macizo Norpatagónico, Río Negro, Argentina. 15th Congreso Geológico Argentino 3: 117-122.

448 Busteros A, Giacosa R, Lema H, Zubia M (1998). Descripción geólogica de la Hoja Sierra Grande (4166-IV),
449 escala 1:250000, provincia de Río Negro. Instituto de Geología y Recursos Minerales, SEGEMAR, Boletín 241,
450 75 p. Buenos Aires.

451 Büttner SH, Glodny J, Lucassen F, Wemmer K, Erdmann S, Handler R, Franz G (2005). Ordovician
452 metamorphism and plutonism in the Sierra de Quilmes metamorphic complex: Implications for the tectonic
453 setting of the northern Sierras Pampeanas (NW Argentina). Lithos 83:143–181.

454 Cagnoni M, Linares E, Ostera H, Parica C, Remesal M. (1993). Caracterización geoquímica de los
455 metasedimentos de la Formación Nahuel Niyeu: implicancias sobre su proveniencia y marco tectónico. 13th
456 Congreso Geológico Argentino and 2nd Congreso de Exploración de Hidrocarburos 1: 281-286. Buenos Aires.

457 Caminos R (1983). Descripción Geológica de las Hojas 39g, Cerro Tapiluke y 39h, Chipauquil, provincia de Río
458 Negro. Servicio Geológico Nacional, (unpublished), 41 p., Buenos Aires.

459 Caminos R (2001). Hoja Geológica N 4166-I Valcheta, provincia de Río Negro, Boletín 310, Servicio Geológico
460 Minero Argentino, 78 p., Buenos Aires.

461 Caminos R, Chernicoff C, Varela R (1994). Evolución tectónico-metamórfica y edad del Complejo Yaminué,
462 Basamento pre-andino norpatagónico, República Argentina. 7th Congreso Geológico Chileno, Actas II: 1301–
463 1305. Concepción.

464 Chernicoff CJ, Caminos R (1996). Estructura y metamorfismo del Complejo Yaminué, Macizo Norpatagónico
465 oriental, provincia de Rio Negro. Revista de la Asociación Geológica Argentina 51: 107-118.

Chernicoff CJ, Zappettini EO, Santos JOS, McNaughton NJ, Belousova E (2013). Combined U-Pb SHRIMP and Hf isotope study of the Late Paleozoic Yaminué Complex, Río Negro province, Argentina: implications for the origin and evolution of the Patagonia composite terrane. Geoscience Frontiers 4: 37-56. DOI 10.1016/j.gsf.2012.06.003.

Croce F, Lince Klinger F, Giménez ME, Martínez MP, Ruiz F. (2009). Estimación de profundidades del Complejo Plutónico Navarrete mediante procesamiento gravimétrico. Geoacta 34: 25-38.

Dahl PS (1996). The crystal-chemical basis for differential argon retention in coexisting muscovite and biotite: Inferences from interlayer partitioning data and implications for geochronology. Contribut Mineral Petrol 123:22-39.

Féraud G, Alric V, Fornari M, Bertrand H, Haller M (1999). The Mesozoic silicic volcanic Province of Patagonia synchronous with the Gondwana Break-up and subduction: spacetime evolution evidenced by $^{40}Ar/^{39}Ar$ data. Earth Planet Sci Lett 172:83-96.

Franzese JR, Spalletti LA (2001). Late Triassic-early Jurassic continental extension in southwest Gondwana: tectonic segmentation and pre-break-up rifting. J S Am Earth Sci 14:257-270.

Giacosa RE (1997). Geología y petrología de las rocas pre-cretácicas de la región de sierra de Pailemán, provincia de Río Negro. Revista de la Asociación Geológica Argentina 52: 71-91.

Giacosa RE (2001). Zonas de cizalla frágil-dúctil neopaleozoicas en el nordeste de la Patagonia. Revista de la Asociación Geológica Argentina 56:131-140.

González SN, Greco GA, González PD, Sato AM, Llambías EJ, Varela R, Basei MAS (2014). Geología, petrografía y edad U-Pb de un enjambre longitudinal NO-SE de diques del Macizo Norpatagónico Oriental, Río Negro. Revista de la Asociación Geológica Argentina 71:174-183.

Gozálvez M (2009)a. Petrografía y edad 40Ar-39Ar de leucogranitos peraluminosos al oeste de Valcheta. Macizo Nordpatagónico (Río Negro). Revista de la Asociación Geológica Argentina 64: 275-284.

Gozálvez M (2009)b. Caracterización del plutón San Martín y las mineralizaciones de wolframio asociadas, departamento Valcheta, provincia de Río Negro. Revista de la Asociación Geológica Argentina 64: 409-425.

491 Greco, GA, González, PD, González, SN, Sato, AM, Basei, MAS, Tassinari, CCG, Sato, K, Varela, R, Llambías,
492 EJ (2015). Geology, structure and age of the Nahuel Niyeu Formation in the aguada Cecilio area, North
493 Patagonian Massif., Argentina. Journal of South American Earth Sciences 62:12-32.

494 Grecco L, Gregori D. (2011). Geoquímica y geocronología del Complejo Plutónico Pailemán, Comarca
495 Nordpatagónica, Provincia de Río Negro. XVIII Congreso Geológico Argentino. 2p

496 Gregori DA, Kostadinoff J, Strazzere L, Raniolo A (2008). Significance and consequences of the Gondwanide
497 orogeny in northern Patagonia, Argentina. Gondwana Res 14: 429-450.

498 Gregori DA, Kostadinoff J, Álvarez G, Raniolo A, Strazzere L, Martínez JC, Barros M (2013). Preandean
499 geological configuration of the eastern North Patagonian Massif, Argentina. Geoscience Frontiers 4: 693-708.

500 von Gosen W. (2003). Thrust tectonics in the North Patagonian Massif (Argentina): implications for a
501 Patagonian plate. Tectonics 22 (1), 1005, doi: 10.1029/2001TC901039.

502 Hansma J, Tohver E, Schrank C, Jourdan F, Adams D. (2015). The Timing of the Cape Orogeny: New $^{40}Ar/^{39}Ar$
503 age constraints on deformation and cooling of the Cape Fold Belt, South Africa. Gondwana Res
504 dx.doi.org/10.1016/j.gr.2015.02.005.

505 Harrison TM, Duncan I, McDougall I (1985). Diffusion of ^{40}Ar in Biotite: Temperature, Pressure and
506 Compositional Effects. Geochim Cosmochim Acta 49: 2461-2468.

507 Harrison TM, Célérier J, Aikman, AB, Hermann J, Heizler M (2009). Diffusion of ^{40}Ar in muscovite. Geochim
508 Cosmochim Acta 73: 1039-1051.

509 Jourdan F, Féraud G, Bertrand H, Kampunzu AB, Tshoso G, Watkeys, MK, Le Gal B (2005). Karoo large
510 igneous province: Brevity, origin, and relation to mass extinction questioned by new 40Ar/39Ar age data.
511 Geology 33: 745-748. doi: 10.1130/G21632.1

512 Kirschner DL, Cosca MA, Masson H. (2003). Timing of deformation in the Helvetic Alps: evidence from
513 $^{40}Ar/^{39}Ar$ and Rb/Sr geochronology of white micas. Contribut Mineral Petrol doi: 10.1007/s00410-003-0461-2.

514 Lince Klinger F, Martínez P, Rapalini AE, Giménez ME, López de Luchi MG, Croce FA, Ruiz F (2010).
515 Modelo gravimétrico en el borde noreste del Macizo Norpatagónico. Revista Brasileira de Geofísica 28:463-472.

516 Lince Klinger F, León M, Martínez P, Weidmann C, Anci S, Álvarez O (2014). Modelo geofísico con datos
517 gravimétricos y aeromagnéticos en el borde noreste del Macizo Norpatagónico, Río Negro, Argentina. Geoacta
518 39:51-61.

519 López de Luchi MG, Rapalini AE, Tomezzoli RN (2010). Magnetic Fabric and microstructures of Late
520 Paleozoic granitoids from the North Patagonian Massif: Evidence of a collision between Patagonia and
521 Gondwana? Tectonophysics 494: 118-137.

522 López de Luchi MG, Martínez Dopico C, Rapalini AE (2013). The Musters Stock: a hybrid quartz monzogabbro
523 to granodiorite, west of Valcheta, Río Negro. 2º Simposio sobre Petrología Ígnea y Metalogénesis Asociada.
524 Resúmenes 49-50. San Luis, Argentina.

525 López de Luchi M, Martínez Dopico C, Rapalini A (2015). Geochemical and isotopic constraints on the sources
526 of the Permian-Early Triassic granitoids of the northeastern sector of the North Patagonian Massif. 3º Simposio
527 sobre Petrología Ígnea y Metalogénesis Asociada. Resúmenes, 49-50. General Roca, Argentina.

528 Ludwig K (2009). Squid 2; A User's Manual. Berkeley Geochronology Center 100p.

529 Ludwig K (2012). User´s Manual for Isoplot 3.75. A Geochronological Toolkit for Microsoft Excel. Berkeley
530 Geochronology Center Special Publication No. 5. 75p.

531 Márquez MJ, Massaferro GI, Fernández MI (2010). El volcanismo del Complejo Marifil en Arroyo Verde,
532 vertiente suroriental del Macizo de Somún Cura, Chubut. Revista de la Asociación Geológica Argentina 66:314-
533 324.

534 Martínez Dopico CI, López de Luchi MG, Rapalini AE (2010)a. Sources for the Ordovician granites in the NE
535 North Patagonian Massif. EOS Trans. AGU, 91(26), Meet. Am. Suppl., Abstract, V11A-07. Foz de Iguazú,
536 Brasil.

Martínez Dopico CI, López de Luchi MG, Wemmer K, Rapalini AE, Linares E (2010)b. Further evidences for the widespread Ordovician Magmatism in the Northeastern North Patagonian Massif: testimony for the continuity of the Famatinian orogen. Bollettino di Geofisica teorica ed applicata 51:34-37.

Martínez Dopico CI, López de Luchi M, Rapalini AE (2014). Petrography and mineral chemistry of the Eraly Paleozoic metamorphic basement north of Valcheta town, Río Negro. XIX Congreso Geológico Argentino. Online files 1p.

McDougall I, Harrison TM (1999). Geochronology and thermochronology by the $^{40}Ar/^{40}Ar$ method. 2nd ed., 269 pp. Oxford University Press, Oxford.

Naipauer M, García Morabito E, Marques J, Tunik M, Rojas Vera EA, Vujovich GI, Pimentel MP, Ramos VA (2012). Intraplate Late Jurassic deformation and exhumation in western central Argentina: constraints from surface and U-Pb detrital zircon ages. Tectonophysics 524-525: 59-75.

Navarrete C, Gianni G, Echaurren A, Lince Klinger F, Folguera A, (2016). Episodic Jurassic to Lower Cretaceous intraplate compression in Central Patagonia during Gondwana breakup. Journal of Geodynamics http://dx.doi.org/10.1016/j.jog.2016.10.001

Pankhurst RJ, Rapela CW (1995). Production of Jurassic rhyolites by anatexis of the lower crust of Patagonia. Earth and Planetary Science Letters 134:23-36.

Pankhurst RJ, Rapela CW, Caminos R (1993). Problemas geocronológicos de los granitoides gondwánicos de Nahuel Niyeu, Macizo Norpatagónico 12th Congreso Geológico Argentino and 2nd Congreso de Exploración de Hidrocarburos 4:99-104.

Pankhurst R, Riley T, Fanning C, Kelley S (2000). Episodic Silicic Volcanism in Patagonia and the Antartic Peninsula: Chronology of Magmatism Associated with the Break-up of Gondwana. J Petrol 41:605-625.

Pankhurst RJ, Rapela CW, Fanning CM, Márquez M (2006). Gondwanide continental collision and the origin of Patagonia. Earth-Sci Rev 76: 235-257.

Pankhurst RJ, Rapela CW, López de Luchi MG, Rapalini AE, Fanning CM, Galindo C (2014). The Gondwana connections of northern Patagonia. Journal of the Geological Society 171: 313-328. DOI: 10.1144/jgs2013-081

562 Purdy JW, Jäger E (1976). K-Ar ages on rock forming minerals from the Central Alps. Memorie degli Istituti di
563 Geologia e Mineralogia dell' Universita di Padova 30:1-31.

564 Ramos VA (1984). Patagonia: ¿Un continente paleozoico a la deriva? 9th Congreso Geológico Argentino, San
565 Carlos de Bariloche 2:311-325.

566 Rapalini AE, López de Luchi M, Martínez Dopico C, Lince Klinger F, Giménez M, Martínez P (2010). Did
567 Patagonia collide against Gondwana in the Late Paleozoic? Insights from a multidisciplinary study of magmatic
568 units of the North Patagonian Massif. Geol Acta 8:349-371. http://dx.doi.org/doi: 10.1344/105.000001577.

569 Rapalini AE, López de Luchi M, Tohver E, Cawood PA (2013). The South American ancestry of the North
570 Patagonian Massif: geochronological evidence for an autochthonous origin? Terra Nova 25:337-342.
571 http://dx.doi.org/doi: 10.1111/ter.12043.

572 Sato AM, Basei MAS, Tickyj H, Llambías EJ, Varela R (2004). Granodiorita El Sótano: plutón jurásico
573 deformado aflorante en el basamento de Las Grutas, Macizo Norpatagónico Atlántico. Revista de la Asociación
574 Geológica Argentina 59:591-600.

575 Steenken A, Wemmer K, López de Luchi MG, Siegesmund S, Pawlig S (2004). Crustal Provenance and Cooling
576 of the Basement Complexes of the Sierra de San Luis: An Insight into the Tectonic History of the Proto-Andean
577 Margin of Gondwana. Gondwana Res 7:1171-1195.

578 Stern RA (2001). A new isotopic and trace-element standard for the ion microprobe: preliminary thermal
579 ionization mass spectrometry (TIMS) U-Pb and electron-microprobe data. Radiogenic Age and Isotopic Studies:
580 Report 14, Geological Survey of Canada, Current Research 2001-F1, 11p.

581 Tohver E, Cawood PA, Rossello E, López de Luchi MG, Rapalini A, Jourdan F (2008). New SHRIMP U–Pb
582 and $^{40}Ar/^{39}Ar$ constraints on the crustal stabilization of southern South America, from the margin of the Rio de
583 Plata (Sierra de Ventana) craton to northern Patagonia. EOS Abstracts, American Geophysical Union, Fall
584 Meeting, T23C-2052.

585 Tohver E, Cawood PA, Rosello EA, Jourdan F (2012). Closure of the Clymene Ocean and formation of West
586 Gondwana in the Cambrian: Evidence from the Sierras Australes of the southernmost Río de la Plata craton,
587 Argentina. Gondwana Res 21:394-405. DOI:10.1016/j.gr.2011.04.001

588 Tommezzoli RN, Rapalini AE, López de Luchi MG, Martínez Dopico CI (2013). Permian remagnetization of
589 Ordovician granitoids in northeastern North Patagonian Massif, Argentina. Gondwana Res 24:192-202.

590 Uriz NJ, Cingolani CA, Chemale Jr F, Macambira MB, Armstrong R (2011). Isotopic studies on detrital zircons
591 of Silurian- Devonian siliciclastic sequences from Argentinean North Patagonia and Sierra de la Ventana
592 regions: comparative provenance. Int J Earth Sci 100:571-589.

593 Varela R, Sato K, González PD, Sato AM, Basei MAS (2009). Geología y geocronología Rb-Sr de granitoides
594 de Sierra Grande, Provincia de Río Negro. Revista de la Asociación Geológica Argentina 64:275-284.

595 Wemmer K (1991). K/Ar-Altersdatierungsmöglichkeiten für retrograde Deformationsprozesse im spröden und
596 duktilen Bereich-Beispiele aus der KTB-Vorbohrung (Oberpfalz) und dem Bereich der Insubrischen Linie (N-
597 Italien). Göttinger Arbeiten zur Geologie und Paläontologie 51:1-61.

598 Zanettini JCM (1980). Sedimentitas Triásicas al sur de Sierra Grande (Provincias de Río Negro y Chubut).
599 Revista de la Asociación Geológica Argentina 35:301-307.

600 Zanettini JCM (1981). La Formación Sierra Grande (provincia de Río Negro). Revista de la Asociación
601 Geológica Argentina 36:160–179.

602

603 **CAPTIONS**

604 **Figure 1.** Geological setting of northeastern Patagonia (North Patagonian Massif) a) Regional map. Localities
605 referred to in the text are indicated; PB, Pampean Belt; FB, Famatinian Belt; PT, Precordillera Terrane; b)
606 Geological map between Valcheta and Nihuel Niyeu towns based on Rapalini et al. (2013) and Pankhurst et al.
607 (2014). The location of the Ar-Ar, K-Ar mica, and U-Pb zircon ages is indicated in blue and black and white
608 bolded ballons, respectively. White ballons correspond to previous U-Pb zircon SHRIMP dating (black text,
609 Pankhurst et al., 2006, 2013; Tohver et al. 2008; Chernicoff et al., 2013; Rapalini et al., 2013) and black ballons
610 represent the detrital maximum depositional ages (Pankhurst et al., 2006; Tohver et al., 2008; Chernicoff et al.,

2013; Rapalini et al., 2013). The black double line represents the contact lineament between the Yaminué block and the Nahuel Niyeu block according to the gravimetrical model of Lince et al. (2010, 2014), Rapalini et al. (2010) and magnetometrical data of Chernicoff et al. (2013).

Figure 2. Results of the combined U-Pb SHRIMP zircon and/or $^{39}Ar/^{40}Ar$ mica ages on samples a) U-Pb Concordia diagram for sample SA100, foliated granodiorite/ tonalite of the southern Yaminué Complex taken from Rapalini et al. (2013); b) $^{39}Ar/^{40}Ar$ spectra of biotite of a foliated granodiorite layer of the southern Yaminué Complex, (sample V79) in the same locality of SA100; c) U-Pb Concordia crystallization age for an undeformed monzogranite of the Cabeza de Vaca Granite (Sample 104); d) Ar/Ar spectra of biotite extracted of the monzogranite of sample SA104 (separate V58); e) U-Pb Concordia crystallization age of a leucogranite dike (sample SA101); f) $^{39}Ar/^{40}Ar$ step heating for the muscovite blasts within the Nahuel Niyeu Formation (sample SA115). Blasts are related to the contact aureole of the Navarrete Granodiorite in Puesto Navarrete locality.

Figure 3: Summary of the new and already published geochronologic data and events for northeastern Patagonia (time is shown in Y-axis in Ma from Cambrian to Jurassic) along a southwest to northeast traverse across the towns of Yaminué, Nahuel Niyeu and Valcheta towns (geological unit X- axis). Geochronological data comprises zircon U-Pb crystallization ages and detrital ages peaks (magmatic ages in rectangles), maximum depositional ages (stars), Ar-Ar and K-Ar cooling ages in biotite, muscovite and whole rock (in circles) and Rb-Sr whole rock isochron (triangles). New ages are labelled as 'N" whereas published ages sources are referred with numbers: 1- Foliated Granodiorite (Rapalini et al. 2013); 2- Bt Paragneiss (Tohver et al. 2008); 3- Bt paragneiss (Chernicoff et al. 2013); 4- Orthogneiss (Chernicoff et al. 2013); 5,6,7- Granite (Pankhurst et al. 2014); 8- Andesite Dike in Mina Gonzalito Area (González et al. 2014); 9- Leucogranite (Pankhurst et al. 1993); 10- Bt tonalite (Pankhurst et al. 2014); 11- Granodiorite (Pankhurst et al. 2006); 12- Bt-Ms granite (Pankhurst et al. 2006, Gozálvez 2008a, López de Luchi et al. 2008); 13- Porphyritic Granite (Rapalini et al. 2013; Pankhurst et al., 20140; 14- Metaclastic rock (Pankhurst et al. 2006; Rapalini et al. 2013); 15- Volcaniclastic level (Rapalini et al. 2013); 16- Ms blast in phyllite; 17- Ms (bt) Granites (Gozálvez et al. 2008a; Rapalini et al. 2013); 18- Ignimbrite/ Rhyolites (Pankhurst et al.1998; Márquez et al. 2012); 19- Magmatic sill in Aguada Cecilio (Greco et al. 2015); 20- Sandstone (Youngest Zircon 428 Ma, Uriz et al. 2011); 21- Conglomerates (Zanettini 1980). Dashed blue line represents the location of the Tardugno Fault. Metamorphic events are marked as swung dashes (ca. 470 Ma-Lower Ordovician- for Mina Gonzalito Complex, further southeast of the studied area

641 (Pankhurst et al., 2006) and late Permian (between 260 and 250 Ma, Chernicoff et al., 2013; Pankhurst et al.,
642 2014, respectively).
643
644 **Figure 4.** Probability density plot and histogram of the detrital zircons U-Pb ages of the metaclastic host of the
645 Yaminué granites obtained in Tohver et al. (2008) (N=28) and Chernicoff et al. (2013) (N= 20). Concordance
646 level is over 90%. Bin width 50 Ma.
647
648 **Table 1.** Summary of mica K-Ar, $^{40}Ar/^{39}Ar$ and zircon U-Pb SHRIMP age results. See the details and analytical
649 data in the text and appendix A and B, respectively.
650
651 **Appendix A:** Ar-Ar and K-Ar analytical data.
652
653 **Appendix B:** U-Pb SHRIMP zircon data.

Figure 1 R2

Click here to download Figure Fig 1 v12 Rev Rev.tif

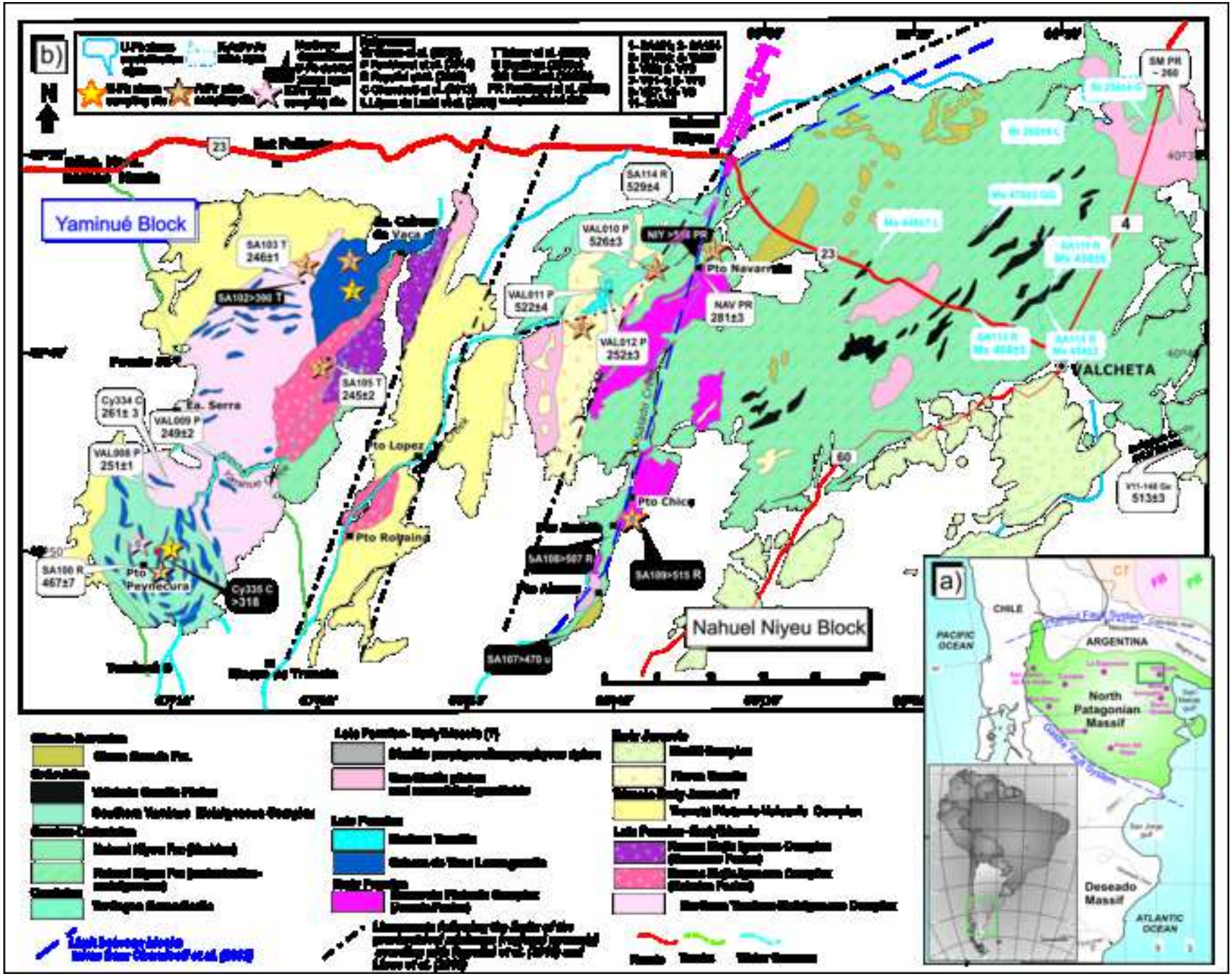

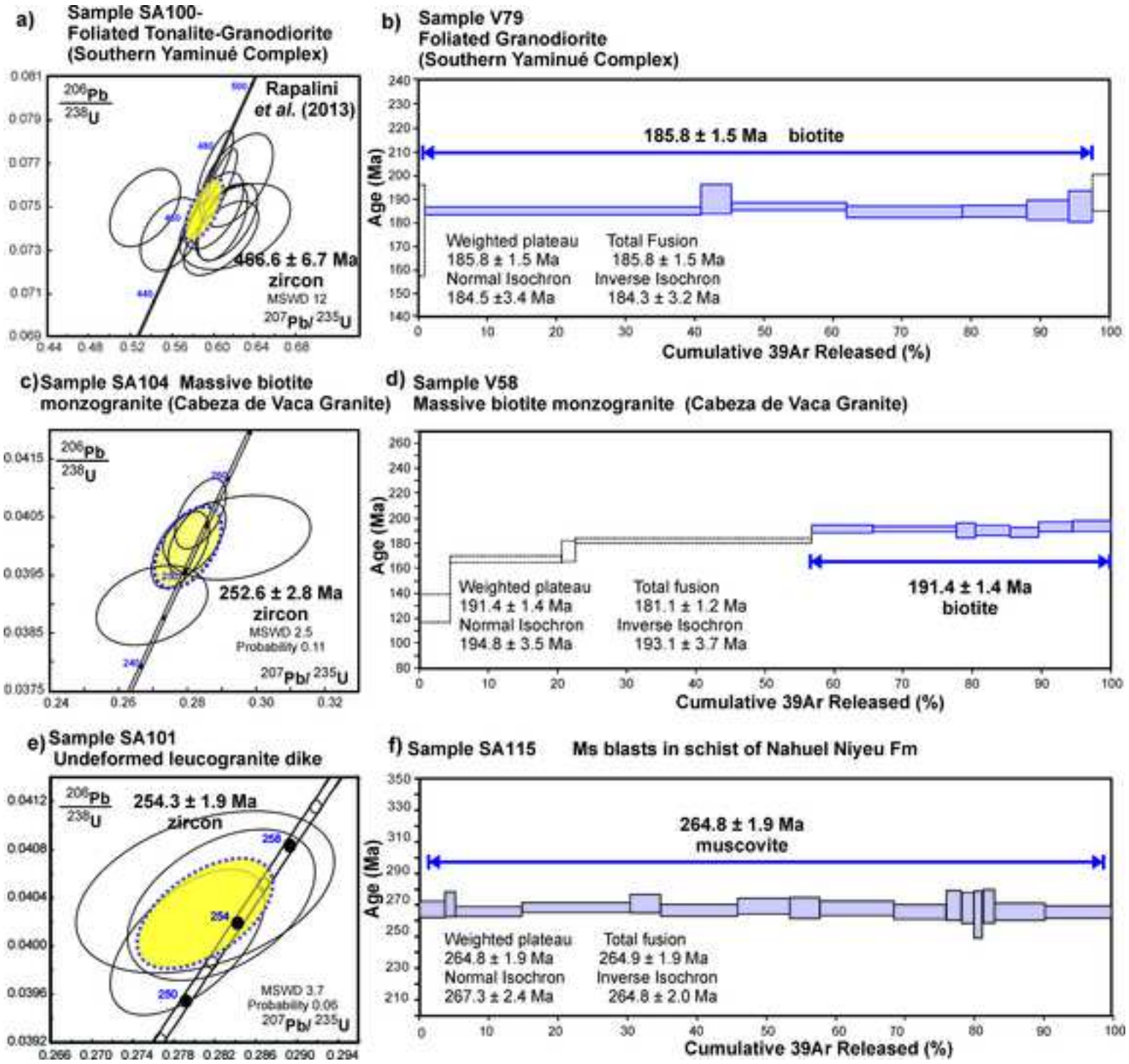

Figure 3 R2

Click here to download Figure figure 3 v 12revrev jul16c.tif

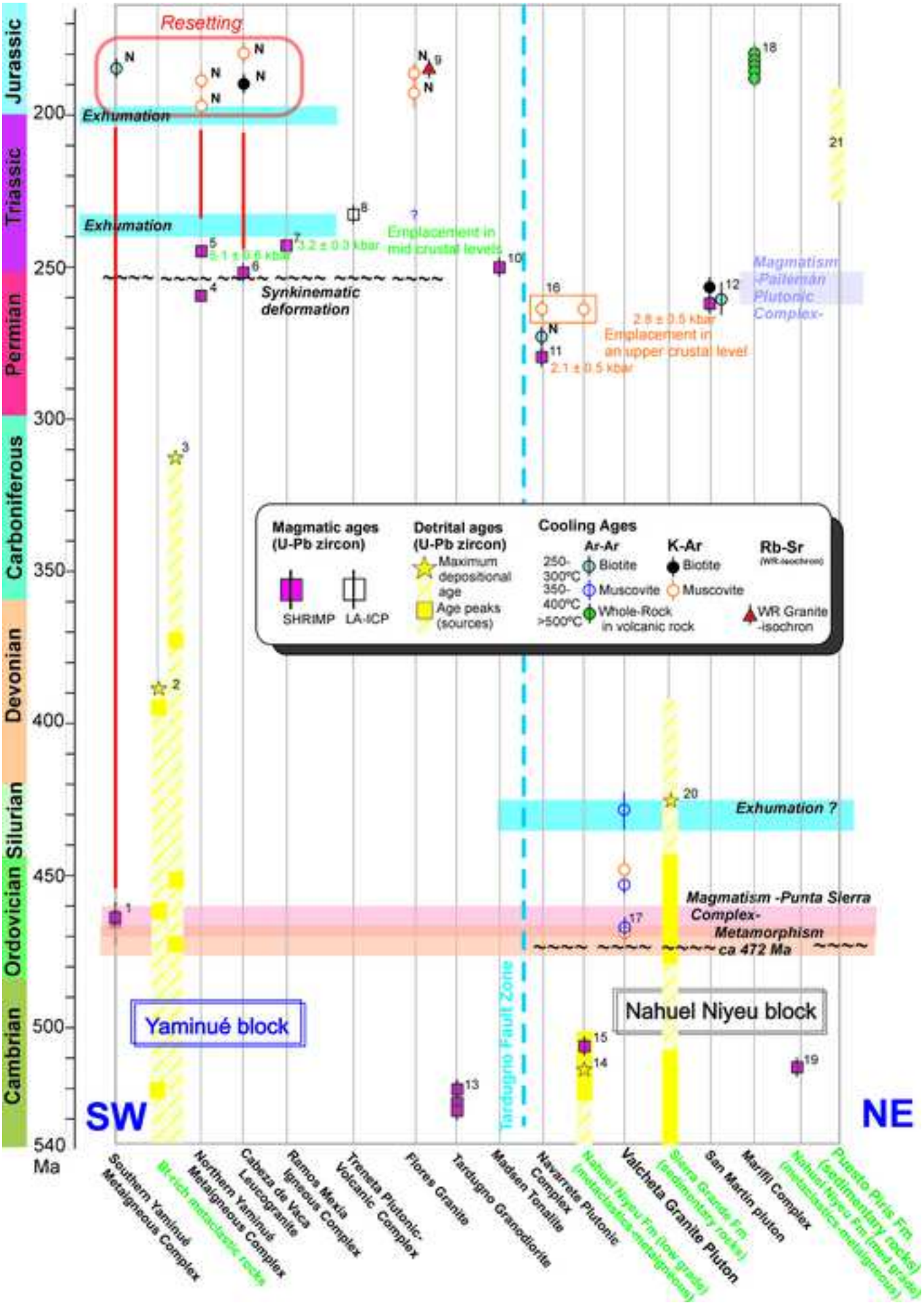

Figure 4 R2

Click here to download Figure figure 4.tif

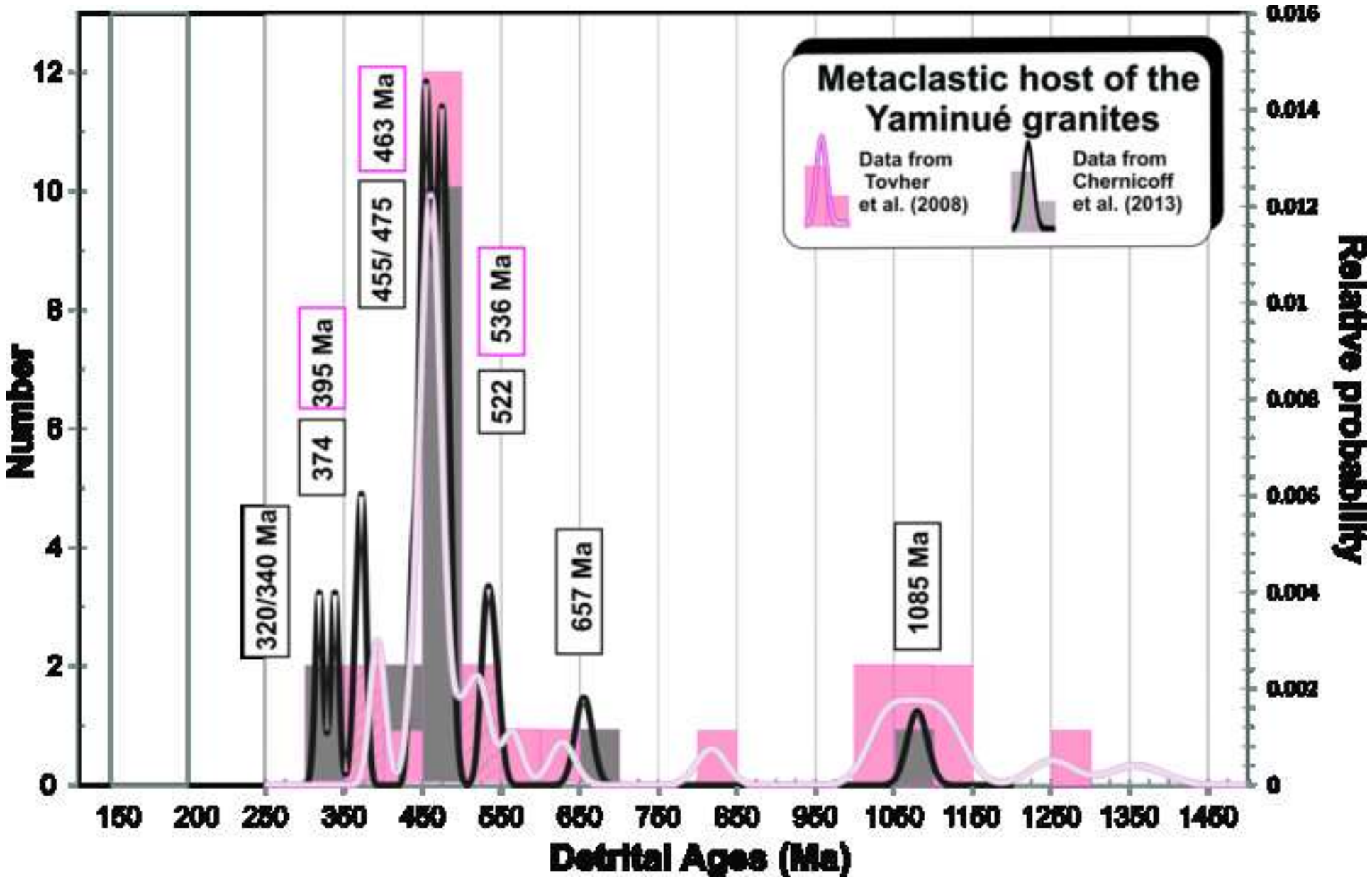

Table 1 R2

	Sample	Mineral	Lithology	Unit	Age [Ma]	2s-Error [Ma]
U-Pb SHRIMP	SA101	Zrc	Slightly deformed leucogranite dike intruding V79	Yaminué Metaigneous Complex (south)	**254.3**	**3.8**
	SA104/ V58	Zrc	Massive bt- granite	Cabeza de Vaca Granite	**252.6**	**5.6**
Ar-Ar	SA115	Ms	Muscovite blasts in phyllite	Nahuel Niyeu Fm	**264.8**	**1.9**
	V58	Bt	Massive bt- granite	Cabeza de Vaca Granite	**191.4**	**1.4**
	V79	Bt	Foliated granodiorite	Yaminué Metaigneous Complex (south)	**185.8**	**1.5**
K-Ar	V75	Ms	Undeformed Monzogranite	Navarrete Plutonic Complex	**274.3**	**4.1**
	V69	Ms	Ms booklets of a miarole of foliated leucogranite dyke discordant with the main facies of the Ramos Mexía Complex	Cabeza de Vaca Granite	**190.1**	**2.0**
	V79-1	Ms	Ms- fine grained-leucogranite dike concordant with the host	Yaminué Metaigneous Complex (south)	**182.4**	**2.9**
	VAL55	Ms	Ms booklets of a miarole of foliated leucogranite dyke	Cabeza de Vaca Granite	**198.2**	**2.2**
	V8E	Ms	Pegmatite in fine grained leucogranite	Flores Granite	**193.3**	**4.5**
	V27b	Ms	Pegmatite in fine grained leucogranite	Flores Granite	**188.2**	**2.9**

	Sample	Mineral	Location -UTM 19G (m) E	S	K2O [Wt. %]	40 Ar * [nl/g]	40 Ar * [%]	Age [Ma]	2s-Error [Ma]
K-Ar	V75	Ms	694721.84	5474430.97	9.71	92.76	97.35	**274.3**	**4.1**
	V69	Ms	666977.79	5495311.79	10.67	68.99	97.08	**190.1**	**2**
	V79-1	Ms	652638.39	5477758.17	10.76	66.6	97.87	**182.4**	**2.9**
	VAL55	Ms	667073.98	5501161.11	10.67	72.11	93.93	**198.2**	**2.2**
	V8E	Ms	701630.06	5503625.41	10.52	69.24	95.53	**193.3**	**4.5**
	V27b	Ms	696415.99	5501265.17	10.54	67.43	98.09	**188.2**	**2.9**
Ar-Ar	SA115	Ms	705633.17	5503762.84	-	-	-	**264.8**	**1.9**
	V58	Bt	671771.72	5504188.83	-	-	-	**191.4**	**1.4**
	V79	Bt	652638.39	5477758.17	-	-	-	**185.6**	**1.5**

Spot	$^{204}Pb/^{06}Pb$	±%	$^{207}Pb/^{06}Pb$	±%	$^{208}Pb/^{206}Pb$	±%	Obs $^{206}Pb/^{238}U$	±%	% common ^{206}Pb	U (ppm)	Th (ppm)	Corr $^{206}Pb/^{38}U$	Age (Ma) $^{206}Pb/^{238}U$ (1)	Age (Ma) $^{207}Pb/^{206}Pb$ (1)	% Discordancy	$^{238}U/^{206}Pb$ r	±%	$^{207}Pb/^{206}Pb$ r	±%	$^{207}Pb/^{235}U$	±%	$^{206}Pb/^{238}U$	±%	err corr	Notes
Sample SA101 (UTM 19G 652638.39E, 5477758.17S) Undeformed dike crosscutting V79																									
SA101-07-01	1.6E-4	35	0.074	0.9	0.109	1.3	0.470	0.8	0.28	295	105	0.169	**1006.0 ±12.5**	965 ±31	-4	5.921	1.3	0.071	1.5	1.659	2.0	0.169	1.3	0.660	Inh
SA101-07-02	1.4E-4	33	0.053	1.2	0.399	0.8	0.117	0.4	0.26	1064	1384	0.040	**253.0 ±3.1**	224 ±43	-11	24.981	1.3	0.051	1.8	0.279	2.2	0.040	1.3	0.564	*
SA101-07-03	2.6E-4	38	0.054	1.7	0.048	3.0	0.114	0.7	0.47	484	59	0.041	**255.6 ±3.4**	213 ±79	-17	24.721	1.3	0.050	3.4	0.281	3.7	0.040	1.3	0.368	*
SA101-07-05	1.7E-4	27	0.073	0.9	0.456	1.0	0.460	1.0	0.30	362	521	0.160	**952.8 ±12.6**	957 ±27	0	6.278	1.4	0.071	1.3	1.559	1.9	0.159	1.4	0.733	Inh
SA101-07-06	8.8E-5	16	0.052	0.3	0.050	0.6	0.157	0.6	0.16	10333	1618	0.047	**296.6 ±3.5**	225 ±13	-24	21.238	1.2	0.051	0.6	0.329	1.3	0.047	1.2	0.904	
SA101-07-07	5.8E-4	25	0.057	2.4	0.326	1.1	0.114	0.5	1.07	671	697	0.037	**234.6 ±3.1**	125 ±128	-47	26.982	1.3	0.049	5.4	0.248	5.6	0.037	1.3	0.238	
SA101-07-08	1.8E-4	33	0.053	1.3	0.468	0.8	0.112	0.9	0.33	822	1215	0.040	**254.9 ±3.2**	232 ±53	-9	24.796	1.3	0.051	2.3	0.282	2.6	0.040	1.3	0.490	*
SA101-07-09	2.0E-3	13	0.072	1.3	0.328	2.6	0.096	2.0	3.61	733	634	0.039	**239.0 ±3.3**	-156 ±253	-165	26.477	1.4	0.043	10.2	0.225	10.3	0.038	1.4	0.136	
SA101-07-10	8.1E-5	44	0.126	0.5	0.028	3.6	0.258	1.0	0.14	1298	108	0.092	**567.6 ±6.9**	2031 ±11	258	10.864	1.3	0.125	0.6	1.589	1.4	0.092	1.3	0.901	
SA101-07-12	7.4E-4	28	0.062	3.0	0.124	2.4	0.211	0.8	1.32	175	66	0.076	**466.5 ±6.9**	252 ±163	-46	13.326	1.5	0.051	7.1	0.530	7.2	0.075	1.5	0.211	
SA101-07-13	1.2E-6	2913	0.058	1.5	0.028	2.5	0.189	0.4	0.00	759	51	0.063	**393.8 ±5.1**	535 ±38	36	15.874	1.3	0.058	1.7	0.505	2.2	0.063	1.3	0.612	
Sample SA104 (UTM 19G 671771.72E, 5504188.83S)- Undeformed biotite monzogranite																									
SA104-07-1	1.3E-4	45	0.052	1.1	0.491	0.8	0.112	0.6	0.24	1179	1814	40.500	**252.3 ±3.3**	219 ±48	-13	25.049	1.3	0.051	2.1	0.278	2.5	0.040	1.3	0.542	*
SA104-07-10	8.3E-5	55	0.060	1.7	0.144	1.2	0.236	0.4	0.15	529	236	39.600	**538.8 ±6.7**	553 ±46	3	11.471	1.3	0.059	2.1	0.705	2.5	0.087	1.3	0.525	Inh
SA104-07-11	2.6E-4	33	0.058	1.3	0.408	0.9	0.115	0.4	0.48	840	1071	30.200	**262.8 ±3.3**	362 ±62	38	24.036	1.3	0.054	2.8	0.309	3.0	0.042	1.3	0.421	
SA104-07-12	1.3E-4	28	0.053	1.3	0.355	0.6	0.124	0.3	0.23	1804	2169	63.000	**256.3 ±3.1**	230 ±39	-10	24.659	1.2	0.051	1.7	0.284	2.1	0.041	1.2	0.587	*
SA104-07-2	5.2E-5	114	0.052	1.1	0.621	0.6	0.118	0.4	0.10	1232	2478	42.500	**253.6 ±3.1**	246 ±47	-3	24.922	1.3	0.051	2.0	0.283	2.4	0.040	1.3	0.522	*
SA104-07-3	1.7E-4	14	0.059	0.9	0.213	0.8	0.196	0.3	0.31	1035	662	58.700	**410.9 ±5.5**	467 ±26	14	15.195	1.4	0.056	1.2	0.511	1.8	0.066	1.4	0.770	
SA104-07-4	2.1E-4	66	0.053	2.0	0.470	1.2	0.112	0.6	0.39	373	573	12.600	**246.5 ±3.5**	203 ±108	-18	25.652	1.4	0.050	4.7	0.270	4.9	0.039	1.4	0.295	*
SA104-07-5	1.3E-4	89	0.058	1.4	0.082	2.0	0.194	0.5	0.24	417	92	23.600	**410.1 ±5.3**	447 ±76	9	15.223	1.3	0.056	3.4	0.506	3.7	0.066	1.3	0.363	
SA104-07-6	3.5E-4	36	0.060	1.9	0.216	2.0	0.211	0.5	0.62	387	234	24.200	**450.2 ±5.9**	422 ±88	-6	13.823	1.4	0.055	3.9	0.551	4.2	0.072	1.4	0.325	
SA104-07-7	5.8E-4	48	0.061	3.2	0.417	2.2	0.111	1.1	1.06	128	165	4.340	**246.5 ±4.2**	311 ±200	26	25.653	1.7	0.053	8.8	0.283	9.0	0.039	1.7	0.195	
SA104-07-8	1.1E-3	30	0.058	3.3	0.649	1.5	0.112	0.9	1.93	181	374	6.330	**252.6 ±4.1**	-197 ±311	-178	25.019	1.7	0.042	12.4	0.234	12.5	0.040	1.7	0.132	
SA104-07-9	3.2E-4	57	0.058	2.3	0.354	1.7	0.111	0.8	0.59	254	281	8.800	**253.8 ±3.7**	336 ±130	32	24.904	1.5	0.053	5.7	0.294	5.9	0.040	1.5	0.251	*

Pb_c and Pb^* indicate the common and radiogenic portions, respectively. (1) Corrected for common Pb using measured ^{204}Pb; *Stars indicate the zircons used in the calculation of Concordia ages. Inh Inherited.